Thickness Induced Structural Phase Transition of Gold Nanofilm

Y. Kondo,[1] Q. Ru,[1] and Kunio Takayanagi[1,2]
[1]*Takayangi Particle Surface Project, ERATO, Japan Science and Technology Corporation, 3-1-2 Musashino, Akishima-shi, Tokyo 196-8558, Japan*
[2]*Department of Material Science and Engineering, Tokyo Institute of Technology, 4259 Nagatsuta, Midori-ku, Yokohama 226-8502, Japan*
(Received 31 August 1998)

Transition of gold (001) nanofilm to a (111) was observed in an ultrahigh vacuum electron microscope. The critical thickness of the nanofilm was measured by electron holography to be eight atom layers. These nanofilms ranged from 2 to 20 nm in length. Analyzing the nanofilms by high resolution electron microscopy and electron diffraction, the lattice spacing of the film was isotropically compressed by 3.1%–3.6%, similar to a hexagonal lattice in 5×20 surface reconstruction. The experiments show that the nanofilm structure is dominated by surfaces. [S0031-9007(98)08307-0]

PACS numbers: 61.16.–d, 61.46.+w, 68.55.–a

In recent years, nanostructures have attracted much interest because of their applications in technologies. In such nanostructures, surfaces should play particularly important roles, since the surface-to-volume ratio becomes increasingly large at nanometer scale length. Phenomena such as wavelength selective fluorescence of porous silicon [1] demonstrates the surface importance.

Surfaces of semiconductors and some metals are well known to be reconstructed. Semiconductors such as Si and Ge have commensurate reconstructions of 2×1 [2], 7×7 [3], and 2×8 [4,5]. Metal surfaces have commensurate-incommensurate reconstructions such as 5×20 of gold (001) [6–8]. Surface reconstruction can change by temperature [9] or by stress [10]. Our interest is in the transformations induced by surface sizes, e.g., 3×1 reconstruction for Au(001) and 5×20 reconstruction on a (001) facet of a fine gold particle [11]. Quite recently, extremely thin gold nanowires [12] have been reported, and even the surface layer of the 2-nm-thick wire was reconstructed; narrow (001) surfaces of the wires have the hexagonal structure similar to the 5×20 reconstruction of the bulk gold (001).

Similar to the gold of fine particles and/or nanowires, films of nanometer scale thicknesses are interesting to study. Particularly the suspended films in vacuum, free from any supporting substrate, are of great interest. If the surface could dominate the bulk, we might anticipate surface-induced spontaneous transition of such thin films. This is also an interesting issue to be answered for future developments in nanoscale science and technology. In this paper, we report structural phase transition of a gold (001) film induced by its thickness. Thinning the (001) film locally by electron beam irradiation, the thin (001) film transformed to a (111) film spontaneously. The (111) film expands laterally over a 10 nm square, until it breaks up. Critical thickness of this transition was estimated to be around 2 nm by electron holography.

The initial gold (001) film was made by vacuum deposition (Pashley's method) [13]. The 3-nm-thick and (500×500)-μm-wide gold film was mounted without glue on a holey carbon film which had degassed by preheating. The UHV electron microscope we used was equipped with a field emission gun and allowed us to view the film under the vacuum level of 3×10^{-8} Pa [14]. The thinning of the gold (001) films was done by intense electron beam irradiation. When the beam had a current density of 100 A/cm^2, the irradiated area was thinned locally through migration of gold atoms from inside to outside of the area [15,16]. The surface of the gold film gave the diffraction pattern of 5×20 reconstruction of gold (001) which indicates the clean surface. We confirmed the temperature change during the thinning process, with indium particles of 100 nm diameter (melting point of bulk indium is 156 °C). The particles did not melt even under a beam current density of 500 A/cm^2. After about 1 h of irradiation the central area of the dip became very thin, 2–3 nm, and the area transformed into the (111) orientation. The transformation over an area of 2 nm^2 was accomplished within 1 sec. The (111) film, then, was expanded laterally as wide as a 10 nm square until it finally broke. There, the thinning process of the (111) film was observed to be layer-by-layer; a (111) step swept the surface one-by-one. Dynamics of the above processes were observed by a TV camera attached to the microscope and recorded on video tape recorders at every 33 ms. In addition to those high resolution electron microscope observations, we made electron diffraction analyses of the film structures intermittently. One noticeable fact, which should be related to the above transition process, is that the present (001) films had 5×20 surface reconstruction until they transformed to the (111) orientation. Details of the structural transition from (001) to (111) film were analyzed after observations on over 80 films.

Figure 1(a) shows a high resolution electron microscope image of an ultrathin (111) film which has been transformed from a (001) film. The (111) film is the rectangular area at the center of the panel being surrounded by the (001) film. A triangular network that appeared at

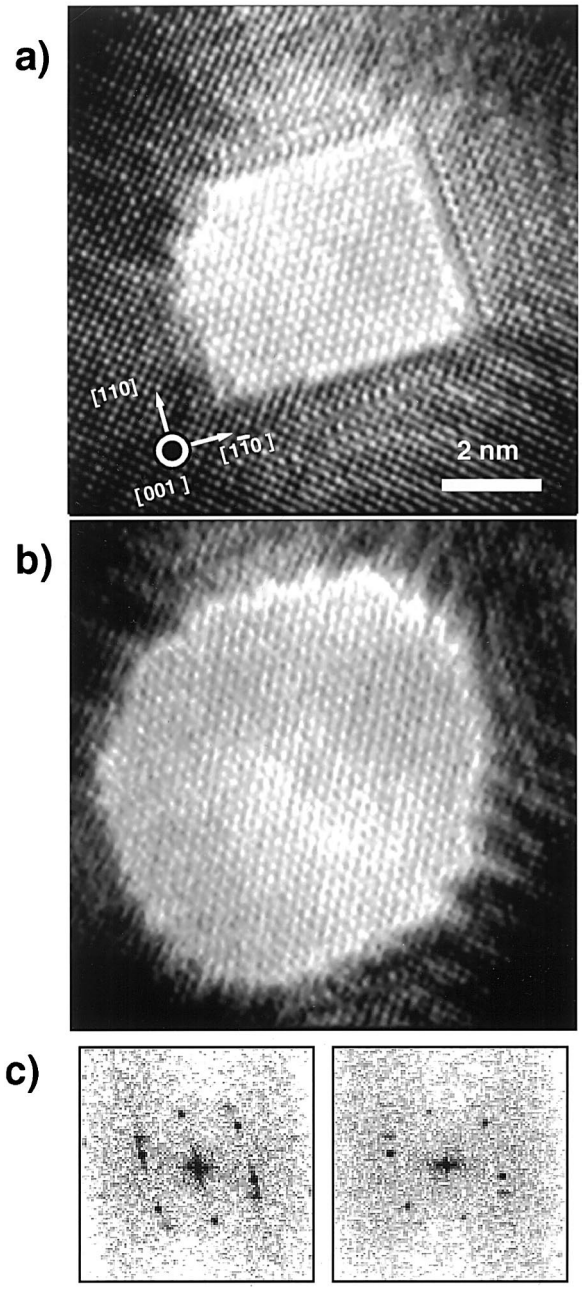

FIG. 1. High resolution electron microscope image of an ultrathin (111) film formed in a (001) film by electron irradiation. (a) The (111) film has a square area. (b) An octagonal area (see Fig. 2). (c) Fourier transform patterns of the image in (a) (left-hand side) and in (b) (right-hand side). The intensity of the imaging electron beam is 30 A/cm^2. The surface of the (001) film has the 5×20 reconstruction. The dark contours marked by arrows are the 2×1 reconstruction on the slopes of {110} surfaces (see Fig. 2).

the central area proves that the hexagonal lattice planes fill this area, but does not prove whether they have the fcc stacking or the hexagonal stacking. We confirmed that these (111) films have the fcc stacking from intensities of the forbidden diffraction spots: $[\frac{2}{3}\,\frac{2}{3}\,\frac{\overline{4}}{3}]$ series. The electron diffraction pattern also showed that no (001) layer has remained within the film. Figure 1(b) is another typical example of the (111) film. This film has an octagonal area, as seen in panel 1(b).

The (111) films in Figs. 1(a) and 1(b) were so uniform that no atomic steps on the surface existed. At the peripheries of these square and octagonal (111) areas, the (111) film changes to the (001) film abruptly. As schematically shown in the film in Fig. 1(b), the (111) film accommodates the sloped (001) film at the abrupt boundaries (see Fig. 2). We suppose that these slopes have {111} and {110} surfaces for the following reasons. First, the square and octagonal areas of the (111) films result because of this geometry. Second, the orientation relation which holds between the (111) and (001) films is explained well, as described later. Third, the dark contour images that appeared at the slope regions could be explained by the 2×1 reconstruction on the {110} surfaces [17].

The orientations of the (001) and (111) films were found, definitely, to be $[1\bar{1}0]_{(001)}//[1\bar{1}0]_{(111)}$ and $[110]_{(001)}//[11\bar{2}]_{(111)}$ in the planes of the films (see Fig. 2). The (111) and (001) films, then, are rotated relatively 35° around the $[\bar{1}10]$ axis, which brings the $[11\bar{2}]$ axis of the (111) film parallel to the [110] axis of the (001) film; the boundary planes between the two films are, then, the 35° tilt and the 35° twist boundaries. Structure of these boundaries is partly seen from high resolution electron microscope images such as shown in Fig. 3. The bright dots in Fig. 3(a) represent hexagonal and square lattices, respectively, of the (111) and (001) films. Bright dots indicate, first, that both films have regular lattices close up to the boundary: Irregular arrangements have one or two atomic widths. Second, both lattices are not coherent, but have misfits in $[\bar{1}10]$ and $[11\bar{2}]$ directions. As is well known from studies on heterogeneous interfaces of thin films, the lattice misfit

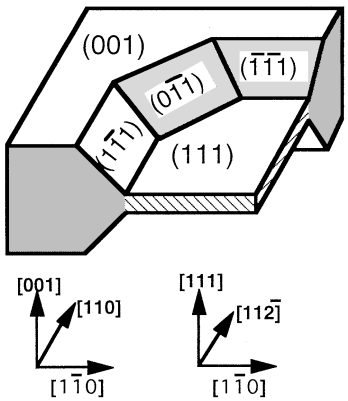

FIG. 2. Morphology of ultrathin (111) film formed in the (001) film. A quarter of the (111) film is shown. The octagonal area of the (111) film is connected by slopes of {110} and {111} surfaces. Crystallographic directions of (001) and (111) films are shown below right and left, respectively.

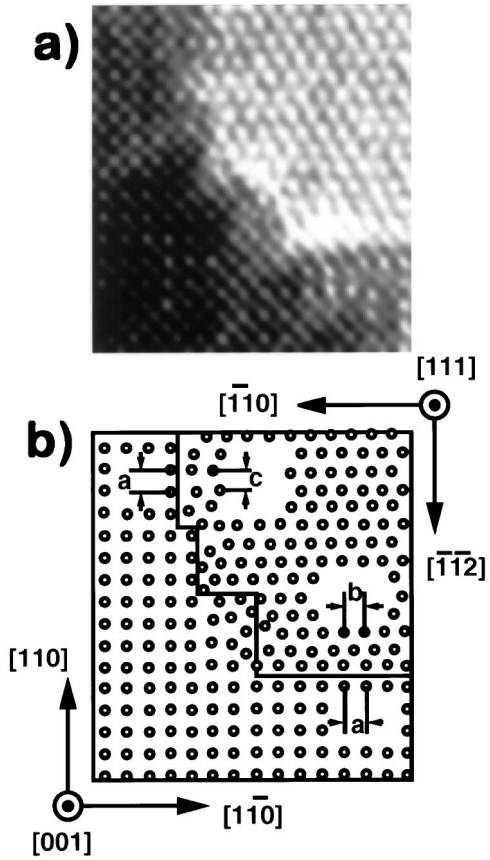

FIG. 3. Structure of the (111) film and boundary with (001) film. (a) High resolution electron microscope image. (b) Trace of the bright dots in (a). The spacings a, b, and c in (b) are of the (110) lattice in the (001) film, (110) and (112) lattices in the (111) film, respectively. The (111) film shrinks as much as $b/a - 1$ in the $[\bar{1}10]$ direction, and $(2/\sqrt{3})(c/a)$ in the $[11\bar{2}]$ direction.

at the interfaces is accommodated by misfit dislocations [18]. Misfit dislocations, after close inspection of the electron microscope image (original photographic film of Fig. 3) and other images of the boundaries, were found to locate not at the boundary plane but at the (001) film of a few atomic distances from the boundary.

Lattice spacings of the (111) and (001) films were, then, analyzed from the electron microscope images such as in Figs. 1(a) and 1(b). All the images showed that the hexagonal lattices of the (111) films were compressed in the $[\bar{1}10]$ and $[1\bar{1}2]$ directions from those of the (111) lattice plane of the bulk crystal; the compressions in these directions are defined by $b/a - 1$ and $(2/\sqrt{3})(c/a) - 1$ [see Fig. 3(b) for definitions of a, b, and c]. More detailed analyses were done by Fourier transforms as shown in Fig. 1(c) of more than 70 microscope images. Since slight correlation between the compressions and the size of the (111) film was found, only histograms of the observed compressions are shown in Figs. 4(a) and 4(b) for the $[\bar{1}10]$ and the $[1\bar{1}2]$ directions, respectively. The average values in these directions were, respectively,

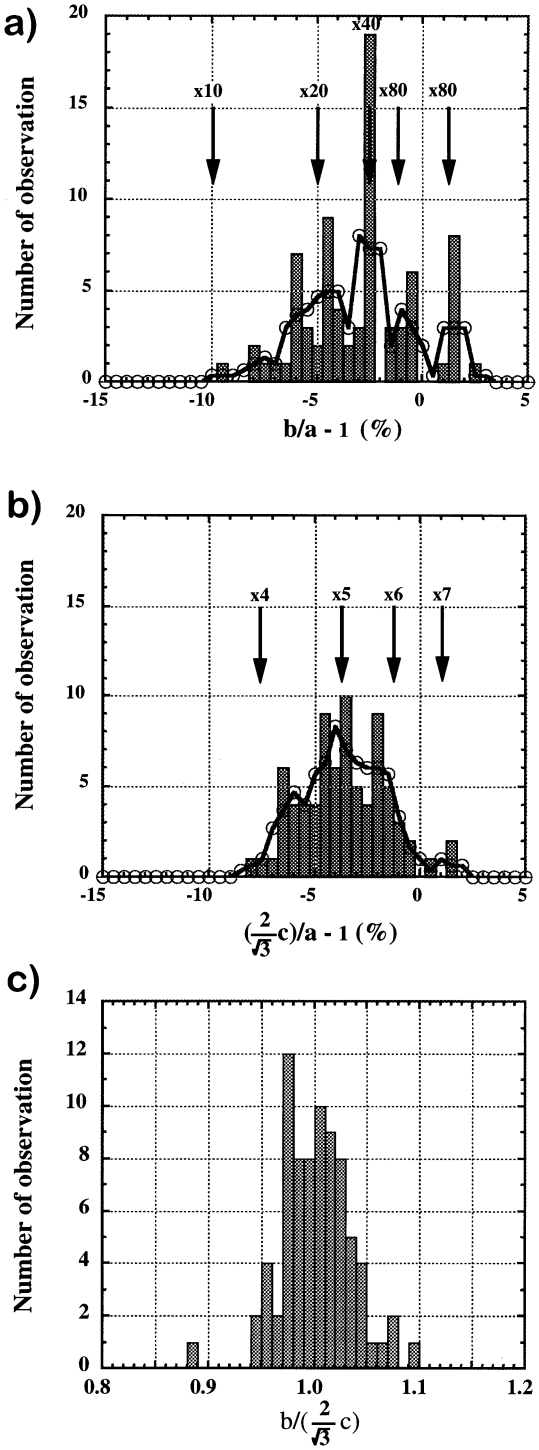

FIG. 4. Histograms of the compressions of the (111) film. (a) Shrinkages in the [110] direction, $b/a - 1$ [see Fig. 3(b)]. The arrows are at -10%, -5%, -2.5%, -1.25%, and $+1.25\%$, for $n = 10$, 20, 40, 80, and -80 of the $n \times m$ coincidence with the (001) lattice. (b) Shrinkages in the $[\bar{1}1\bar{2}]$ direction, $c/a - 1$. The arrows are at -7.6%, -3.8%. -1.2%, and 1%, respectively, for $m = 4$, 5, 6, and 7 of the $n \times m$ coincidence. (c) Ratio of the [110] shrinkage to the $[\bar{1}1\bar{2}]$ shrinkage for each (111) film, $(2/\sqrt{3})(c/b)$. The 20×5 and 40×6 coincidences give 0.99.

3.6% and 3.1%. In the case of a 5×20 reconstructed surface, the hexagonal lattice shrinks in these directions by 5% and 3.8%, respectively. Therefore, we may conclude that the (111) films shrink similarly to the hexagonal lattice in the Au(001) 5×20 reconstruction. We estimate the errors of measurement to be 0.5%–1%. Taking this error into account, the histograms were smoothed and shown by curves in Figs. 4(a) and 4(b). We notice here that histograms in Figs. 4(a) and 4(b) are multiply peaked. These peaks are in accordance with the compressions for $n \times m$ reconstructions ($n = 4$, 5, 6, and 7, and $m = 10$, 20, 40, and 80). Therefore, coincidences of the hexagonal and the square lattices, at the boundaries of the (111) and (001) films, seem to lock the shrinkage. Figure 4(c) shows a histogram for the ratio between the shrinkages in the b and c directions of each (111) film. The peak around 1.0 indicates that the hexagonal lattices shrink isotropically (directional anisotropy is measured to be 1% from Gaussian fitting to the histogram). Thus, we conclude that the (111) film, if it stands free from the (001) film, isotropically shrinks by 3%–4%.

We discuss the threshold which make this transition spontaneous. Before the transition, there exists an interfacial energy originated from the lattice mismatch between the hexagonal surface layer and the subsurface (001) film. After the transition, the (111) film yields a boundary energy with the surrounding (001) film. Since the surface layer of the transformed (111) film has almost the same contraction as the hexagonal surface layer on the (001) film, the energy differences at the transition are the interfacial energy and the boundary energy. Provided that the interfacial energy per unit area is σ, and the boundary energy per unit area is γ, the energy decreases by $\sigma L^2 - \gamma HL$ through the transition, where H is the film thickness, and L is the size of the (111) film. This energy decrease certainly drives the transition. Once the (001) film has transformed to the (111) film, the film becomes stable as it expands laterally. The smallest size of the (111) film after the transition was 2×2 nm^2. The largest size before the break of the film was 24×14 nm, among 80 films observed so far. We determined the thickness to be 1.9 nm for the (111) nanofilm, just after the transition at a size, 4×3 nm^2. There we used electron holography, and assumed a mean inner potential to be 30 eV [19]. Even if a slight uncertainty of the mean inner potential might exist, the thickness must be of the order of eight-(111)-layers-thick [the (111) layer of gold has 0.235 nm spacing]. Below this thickness, no (001) film can survive standing free in vacuum. In other words, gold (001) films are forced to transform by hexagonally reconstructed layers on the top and bottom surfaces. In this respect, it is reasonable that the experiments done on thin (110) films, instead of the (001) film, did not yield (111) films. In addition to the lattice misfit energy, the surface energy of the film decreases after this transition.

In conclusion we found the spontaneous transition of the gold (001) film into the (111) film. The (111) films were compressed isotropically by 3%–4%, similar to the 5×20 reconstructed layer on the gold (001) surface. The critical thickness for this transition was determined by electron holography to be about 2 nm. Eight layers, thus, found to be critical for the gold (001) films, stay stable. This spontaneous transition is forced by the (111)-like reconstruction of the (001) surface.

We believe that this study gives a promising aspect of ultrathin films for designing and fabrication of nanostructures in future technologies.

[1] L. T. Canham, Appl. Phys. Lett. **57**, 1046 (1993).
[2] K. C. Pandy, Phys. Rev. Lett. **47**, 1913 (1981).
[3] K. Takayanagi *et al.*, Surf. Sci. **164**, 367 (1985).
[4] P. W. Palmberg and W. T. Peria, Surf. Sci. **6**, 57 (1967).
[5] T. Ichikawa and S. Ino, Surf. Sci. **105**, 395 (1981).
[6] M. A. Van Hove *et al.*, Surf. Sci. **103**, 189 (1981).
[7] K. Yamazaki *et al.*, Surf. Sci. **199**, 594 (1988).
[8] V. Fiorentini, M. Methfessel, and M. Schoffler, Phys. Rev. Lett. **71**, 1051 (1993).
[9] T. Tabata *et al.*, Surf. Sci. **179**, L63 (1987).
[10] R. J. Hamers, R. M. Tromp, and J. E. Demuth, Phys. Rev. B **34**, 5343 (1986).
[11] M. Mitome and K. Takayanagi, Phys. Rev. B **42**, 7238 (1990).
[12] Y. Kondo and K. Takayanagi, Phys. Rev. Lett. **79**, 3455 (1997).
[13] D. W. Pashley and A. E. B. Presland, J. Inst. Math. Appl. **92**, 297 (1958).
[14] Y. Kondo *et al.*, in *Electron Microscopy and Analysis 1997*, edited by J. M. Rodenburg, Institute of Physics Conference Series Vol. 153 (Institute of Physics Publishing, Bristol, 1997), p. 241.
[15] D. Cherns, Philos. Mag. **36**, 1429 (1977).
[16] K. Niwase *et al.*, Philos. Mag. Lett. **74**, 167 (1996).
[17] S. P. Withrow, J. H. Barrett, and R. J. Culburtson, Surf. Sci **161**, 584 (1985).
[18] J. H. van der Merwe and C. A. B. Ball, *Epitaxial Growth* (Academic Press, New York, 1975), Chap. 6, Pt. B, p. 510.
[19] K. Yada, J. Crystallogr. Soc. Jpn **17**, 226 (1975).